

SECTION 1 PHYSICS OF RADIATION DAMAGES AND EFFECTS IN SOLIDS

<https://doi.org/10.46813/2023-147-003>

UDC 669.017:539.16

HARDENING OF LIGHTWEIGHT MULTI-PRINCIPAL ELEMENT TITANIUM-BASED ALLOY UNDER Ar ION IRRADIATION

*G. Tolstolutska, M. Tikhonovsky, O. Velikodnyi, S. Karpov, V. Ruzhyskiy,
G. Tolmachova, R. Vasilenko*

National Science Centre “Kharkov Institute of Physics and Technology”, Kharkiv, Ukraine

E-mail: g.d.t@kipt.kharkov.ua

Among new prospective materials multi-principal element alloys (MPEA) have attracted considerable attention in recent years due to their excellent corrosion and irradiation resistance as well as their good mechanical properties over a wide temperature range. The new lightweight multi-principal element titanium-based alloy 61Ti-10Cr-7Al-11V-11Nb (at. %) with high ductility at room and elevated temperatures is studied. This single-phase bcc alloy was irradiated with 1.4 MeV Ar ions at room temperature and mid-range doses from 1 to 10 displacements per atom. The effect of irradiation is studied by examining the hardening. A comparison was performed with irradiation-induced hardening behaviour of MPEA, 316 austenitic stainless steel irradiated under an identical condition. It was shown that hardness increases with irradiation dose for all the materials studied, but this increase is lower in multi-principal element alloys both face-centered cubic (FCC) and body-centered cubic (BCC) structures than in stainless conventional steel.

INTRODUCTION

Recently, there has been a growing focus on high-entropy alloys (HEAs) or multi-principal-element alloys (MPEAs), representing a novel class of metallic materials. This emerging field of research is attracting considerable attention within the metallic materials community [1–5]. Latest studies have highlighted that certain HEAs demonstrate superior resistance to irradiation when compared to conventional alloys. This includes enhanced swelling resistance, reduced dislocation evolution, significant reduction in damage accumulation and so on [6–10]. As a result of these findings, HEAs became promising candidates that meet the demanding criteria of complex environments encompassing high temperatures, corrosive conditions, and intense irradiation exposure.

Among the potential applications of MPEAs, a particularly promising one lies in the creation of high-temperature structural materials. Initially developed MPEAs, known as Refractory High Entropy Alloys (RHEAs), exhibited remarkable strength up to 1600 °C; however, they suffered from a notable weight disadvantage. As an alternative approach, novel MPEA alloys based on the Al-Cr-Nb-Ti-V system were developed with the primary goal of decreasing overall density.

Within the context of feasibility studies of advanced nuclear systems, radiation-induced swelling and hardening are key areas of focus. Swelling can be very severe in materials which are not suited for nuclear applications. Similarly, hardening poses a risk to the structural integrity of nuclear materials, potentially causing catastrophic component failure in unfavorable conditions [11].

The response of HEAs as structural materials within the irradiation environments of various nuclear facilities

can be determined by analyzing the effects of proton, heavy ion, neutron, electron, and other particle irradiation damage on HEAs. This approach provides a practical means of evaluating structural materials for use in nuclear facilities. However, there is a deficiency in the existing literature on irradiation-resistant HEAs, as it mainly focuses on equal molar ratio HEAs with a single face-centered cubic (FCC) structure [12]. The irradiation response of non-equal molar ratio HEAs with a body-centered cubic (BCC) structure has received limited investigation.

A brief overview [13] presents the data on recent developments in the field of strong and ductile non-equiatomically high-entropy alloys. It focuses on three key aspects of such non-equiatomically HEAs with excellent strength–ductility combination: thorough exploration of phase stability-driven design, cost-effective and controlled bulk metallurgical processes to achieve suitable microstructures and compositional uniformity, and the resulting microstructure-property correlations. Beyond the principal substitutional elements commonly employed in these alloys, the incorporation of minor interstitial alloying elements is also taken into consideration. The study demonstrates that by shifting the alloy design strategy from single-phase equiatomically compositions to dual- or multiphase non-equiatomically configurations guided by deliberate phase instability, various groups of strong and ductile HEAs can be obtained. This approach opens up opportunities to simultaneously engage multiple strengthening and toughening mechanisms.

This study examines the effect of ion irradiation on the hardening behavior of a new lightweight titanium-based alloy, designated as 61Ti-10Cr-7Al-11V-11Nb (at. %), with a non-equal molar ratio and a homogeneous single-phase BCC structure. The study

also compares the irradiation-induced hardening of this alloy with that of FCC HEAs, 316 austenitic stainless steel all subjected to the same irradiation conditions.

1. MATERIALS AND METHODS

Alloy 61Ti-10Cr-7Al-11V-11Nb (at.%), hereinafter referred to as Ti-MPEA, was obtained by arc melting using a non-consumable tungsten electrode in a pure argon atmosphere. The purity of the initial components was not less than 99.9%. To equalize the chemical composition, the cast alloys were homogenized at a temperature of 1100 °C for 1 h in pure argon, followed by quenching in air. More details on the methods of alloy production and the examination of its structure and properties are given in [14]. Samples for irradiation and subsequent studies were made from the obtained ingots using wire-cut electrical discharge machining. Surfaces of the Ti-MPEA samples were mechanically polished initially with sandpapers of varying grits and finally electrolytically polished using 95% methanol and 5% perchloric acid solution at a temperature of -30 °C with an applied voltage of 20 V.

Samples with dimensions of 10×5×0.5 mm were irradiated with 1.4 MeV argon ions at room temperature (RT) in a dose range of 1...10 dpa. These mid-range doses are evaluated at a depth of ~0.25 μm. All irradiations were carried out with accelerating-measuring system “ESU-2” [15], which contains Van de Graaf accelerator. The depth distribution of Ar atoms concentration and damage was calculated by SRIM 2008 [16] and shown in Fig. 1. According to suggestions of Stoller et al. [17], the quick Kinchin-Pease mode was adopted in this simulation and the displacement energy was set to 40 eV for all target elements.

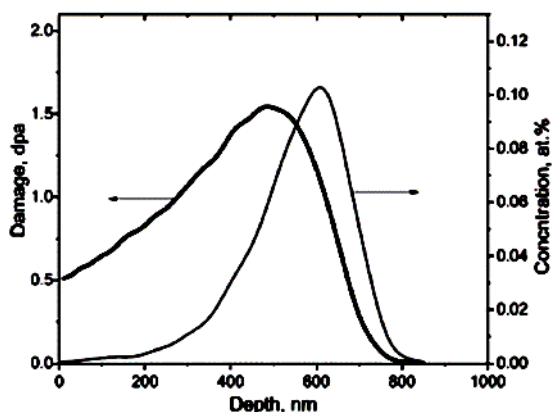


Fig. 1. Calculated profiles of damages and concentrations of 1.4 MeV Ar ions in 61Ti-10Cr-7Al-11V-11Nb alloy to a dose of $1 \cdot 10^{16} \text{ cm}^{-2}$

Nanohardness was measured by Nanoindenter G200 with a Berkovich type indentation tip. A “continuous stiffness measurement method” was used [18], which produces mechanical property data as a function of indenter depth. Tests were performed with a constant deformation rate of 0.05 s^{-1} . Each sample was applied at least 10 prints at a distance of 35 μm from each other. The methodology of Oliver and Pharr was used to find the hardness [19]. The analytical approach for nanoindentation measurement relies on the Nix-Gao

model [20], which introduces the concept of geometrically necessary dislocations needed to accommodate the indenter.

Secondary electron images produced in scanning electron microscopy (SEM, JEOL, JSM-6710F) was used for investigations of as received and irradiated specimens in regions surrounding indents.

2. RESULTS AND DISCUSSION

The initial pre-irradiation microstructure of 61Ti-10Cr-7Al-11V-11Nb alloy is shown in Fig. 2. XRD analysis of alloy have been shown that Ti-MPEA has a single BCC structure without a second phase. Analysis of peaks' FWHMs shows that annealed alloys are in the coarse-grained state. Grains of 60...70 μm in size were fabricated. More details on the initial structure and mechanical properties of alloy are given in [14].

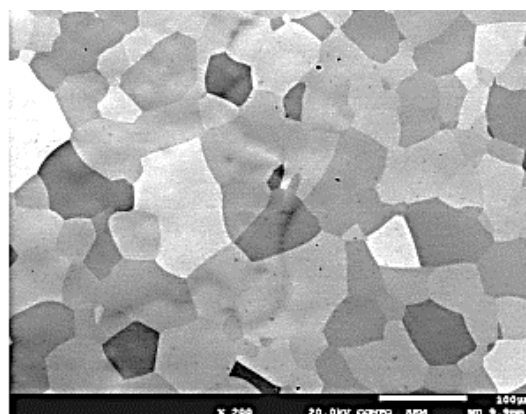


Fig. 2. Initial pre-irradiation microstructure of 61Ti10Cr7Al11V11Nb alloy

Fig. 3 shows nanoindentation hardness (H) as a function of indenter displacement (h) of the unirradiated and irradiated 61Ti-10Cr-7Al-11V-11Nb alloy. The irradiation of alloy with Ar ions at RT leads to an increase of nanohardness.

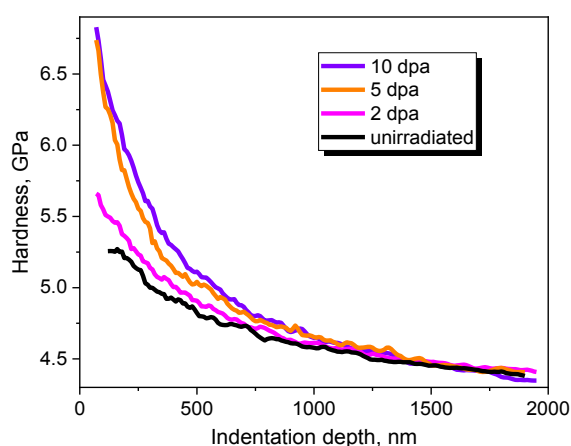


Fig. 3. Nanoindentation hardness versus indentation depth measured for the unirradiated and irradiated specimens

In all samples, the first 150 nm of displacement displays a notable rise in data variability attributed to tip-rounding artifacts and surface preparation influences. Consequently, this first 150 nm of data will be excluded for the subsequent analysis in all samples.

Typically, the indentation hardness of materials subjected to ion irradiation is a result of the combined effects of bulk hardness, the indentation size effect (ISE), and the hardening induced by irradiation [21, 22]. Additionally, the method proposed by Kasada et al. [23] expands upon the Nix-Gao model [20], incorporating a film-substrate system based on the “soft substrate effect”. As outlined in [23], ion-irradiated materials can be considered as systems composed of a “hardened layer-substrate”. The non-irradiated region beneath the irradiated area experiences plastic deformation before the indenter contacts it directly. The point of transition from one region to the other defines the critical indentation depth, denoted as h_c . The bulk equivalent hardness, H_0^{irr} , of the ion irradiated region is determined through a least square fitting of the hardness data up to the critical depth h_c .

By replotting the hardness profile using a Nix-Gao approach, where squared hardness is plotted against reciprocal depth, the evaluation of bulk-equivalent hardness for the ion-irradiated region was performed at irradiation fluences ranging from 2 to 10 dpa (Fig. 4). In the case of the non-irradiated alloy, the Nix-Gao plot appears as a nearly straight line due to the absence of a radiation-hardened layer. The corresponding bulk equivalent hardness, denoted as $H_{0as-received}$, was calculated to be 4.36 GPa. For irradiation doses of 2, 5, and 10 dpa, the determined values of H_0^{irr} were 5.2, 5.4, and 5.6 GPa, respectively.

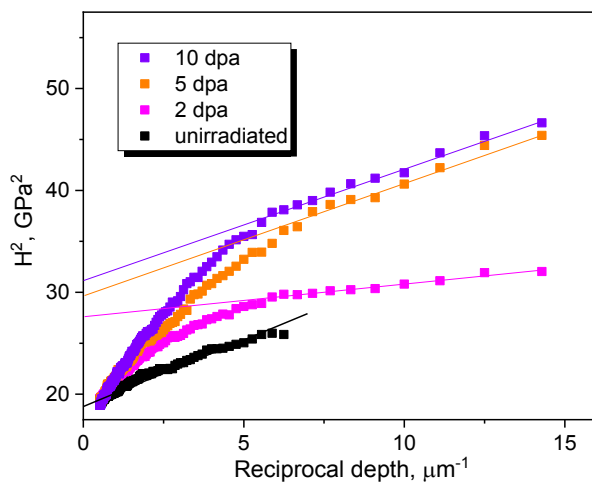


Fig. 4. Nix-Gao plot for unirradiated and argon irradiated 6Ti-10Cr-7Al-11V-11Nb alloy

Following the indentation, SEM imaging was employed to visualize the hardness impressions. As shown in Fig. 5, the observed contours exhibit well-defined straight lines, suggesting the absence of any significant elastic recovery of the indentation sides. Given the small degree of pile-up observed around the indents for both unirradiated and irradiated samples, a correction for contact area was not considered necessary.

The pyramidal shape of the impressions remained consistent for all irradiated samples, implying an isotropic distribution of the compressive load. At the same time, shear-off steps can be seen in the vicinity of the impressions, indicating localized plastic deformation. The shear-off steps are different for grains

with different crystallographic orientations. This behavior is similar to that reported for metallic glasses [24].

In the general case, irradiation-induced hardening exhibited dose-dependent behavior at lower doses and reach saturation at doses exceeding a certain value. Fig. 6 shows the dose dependences of bulk-equivalent hardness for as-received and irradiated Ti-MPEA.

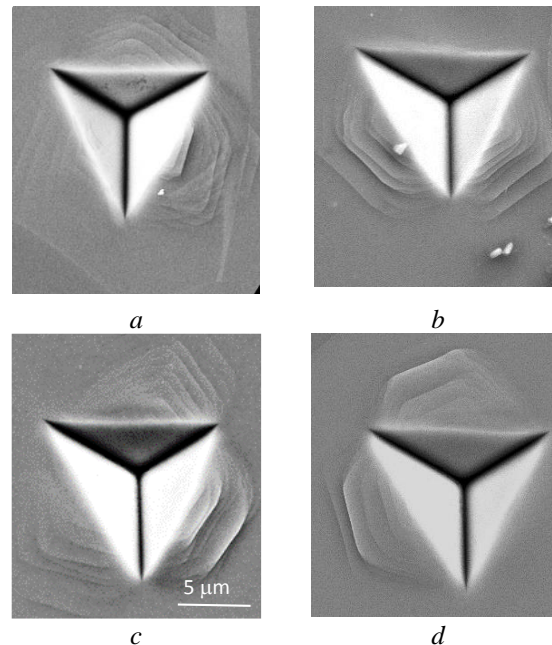


Fig. 5. SEM images showing region of nanoindentation (a) and deformed regions surrounding indents in un-irradiated (a, b) and irradiated (c, d) regions

Irradiation-induced hardness data for previously examined materials such as commercial Type 316 stainless steel (FCC) [25], 20Cr-40Fe-28Mn-20Ni HEA (FCC) [26], are also shown in this figure for comparison.

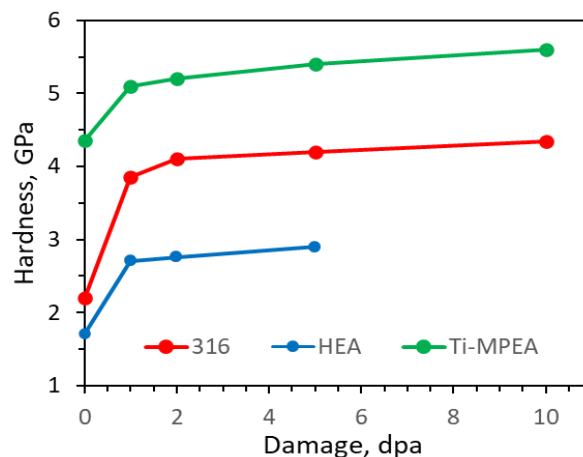


Fig. 6. The dose dependences of bulk-equivalent hardness for as-received and irradiated Ti-MPEA and SS316 and HEA 20Cr-40Fe-20Mn-20Ni for comparison

As evident from Fig. 6, the most pronounced irradiation effect is observed at a dose of approximately 1 dpa, with a gradual transition toward a quasi-saturation mode at higher fluences. Notably, G.S. Was

et al., in their analysis of radiation-induced hardening data for identical heats of proton- and neutron-irradiated 304SS and 316SS, have demonstrated that the radiation hardening of austenitic steels saturates after a few dpa [27].

A comparison of radiation hardening, denoted as $\Delta H = H_0^{irr} - H_0^{as-received}$, was conducted between Ti-MPEA and the aforementioned reference materials, all irradiated under identical conditions (Fig. 7).

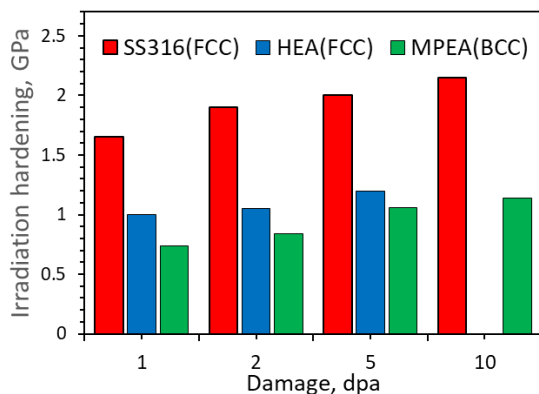


Fig. 7. The radiation hardening $\Delta H = H_0^{irr} - H_0^{as-received}$ versus damage

The interpretation of the data shown in Figs. 6 and 7 should involve the following considerations. The BCC-phase Ti-MPEA exhibits exceptionally high intrinsic hardness even prior to irradiation. Meanwhile, the magnitude of radiation hardening for ion-irradiated Ti-based MPEA and FCC-HEA was significantly smaller compared to SS316.

In general case, the increase in hardness can be explained by commonly accepted models [28–31] which imply the presence of irradiation defect clusters, such as dislocation loops, acting as obstacles to the glide of dislocations.

In all metallic materials, ion irradiation displaces the atoms from their position and leads to point defects formation. However, the multi component alloys have some features, such as high mixing entropy effect in thermodynamics, lattice distortion effect in structure, which appear to be responsible for the lower defect density in HEAs compared to the steel. In addition, the primary mechanism responsible for recovery in high-entropy alloys has been identified as the recombination of vacancies and interstitials, which can be attributed to the increased complexity in the composition and the differences in atomic sizes between the principal elements comprising the alloy [32].

Some atomistic simulations and experimental findings also indicate, that suppression of accumulated damage level in more complex and disordered alloys may be attributed to modified migration barriers and limited atomic diffusion [33, 34]. The energy barrier for an atom to move between positions with different lattice potential energies can make this process energetically unfavorable, leading to a decrease in the overall mobility of interstitials and vacancies, hindering the formation and growth of vacancy clusters and dislocation loops, while promoting the recombination of vacancy-interstitial pairs.

Although radiation-induced hardening in metals is generally associated with the formation of dislocation loops which greatly impede the movement of dislocations, an additional hardening effect can be attributed to the radiation-induced cavity formation. In the present study, the accumulation of noble gas atoms as a result of 1.4 MeV Ar⁺ implantation can promote the nucleation and growth of nano-sized bubbles, which can strongly influence the hardening behavior of the material.

Particularly, argon-filled nanocavities have been found to exhibit a clear tendency to increase in the barrier strength with decreasing in cavity size in the case of Ar-irradiated stainless steel [35–39].

A detailed microstructure examination of irradiated specimens, which is currently underway, is expected to facilitate to the identification of the hardening mechanisms in the Ti-based MPEA alloy.

A comprehensive overview of the results of irradiation hardening behavior for a wide range of HEA materials has been recently presented in [40]. Fig. 8 shows a comparison between the irradiation hardening observed in the current study and the findings reported by other researchers [40]. Notably, previous investigations on HEAs concerning the effects of irradiation hardening have focused on the irradiation damage up to 20 dpa. This value is considerably lower than the prescribed specifications for future advanced nuclear energy systems, which target around 200 dpa. However, it is noteworthy that a significant increase in hardness rapidly occurs within the range of several dpa for a wide range of materials studied. As the irradiation dose increases further, the hardening process gradually approaches saturation.

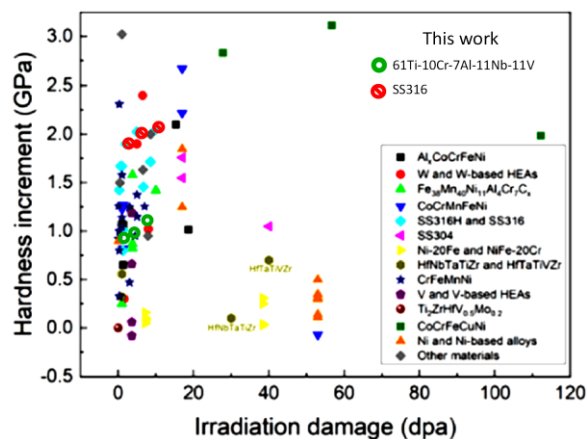


Fig. 8. Irradiation hardness increment, ΔH , versus irradiation damage. The data for comparison is taken from [40]

Analysis of Fig. 8 reveals that the irradiation-induced hardening observed in certain BCC-phase HEAs is notably lower than that observed in both FCC-phase HEAs and conventional alloys such as SS304 and SS316. This discrepancy suggests that certain BCC-phase HEAs exhibit higher resistance to irradiation hardening than conventional alloys. This advantage can be attributed to the higher stacking fault energies and greater lattice distortion in BCC-phase HEAs than in their FCC-phase HEA counterparts.

Meanwhile, some BCC-phase HEAs, as well as the studied Ti-based MPEA alloy, have extremely high intrinsic hardness even before irradiation, and may have brittle fracture behavior. However, the results obtained in the present work are located in the general band of available data and are in good agreement with the results obtained by other authors in terms of the tendency of better resistance to hardening and, consequently, reduced embrittlement of materials with BCC structure, especially HEAs with BCC-phase.

CONCLUSIONS

The new lightweight multi-principal element titanium-based alloy 61Ti10Cr7Al11V11Nb (at. %) with non-equal molar ratio and a homogeneous single-phase BCC structure was used to measure the ion irradiation effect on hardening after irradiation with 1.4 MeV Ar ions at room temperature. The following conclusions were drawn:

BCC-phase Ti-MPEA shows high intrinsic hardness even before irradiation. Radiation-induced hardening of Ti-MPEA is most pronounced at a dose of about 1 dpa, with a gradual approach to quasi-saturation at higher fluences.

The magnitude of hardening for ion-irradiated multi-principal element alloy was significantly smaller compared to SS316. This may be due to the different type and density of defects generated in the MPEA after irradiation compared to conventional nuclear materials such as SS316.

Ti-MPEA with a homogeneous single-phase BCC structure has demonstrated its potential advantages compared to 316 austenitic stainless steel and FCC HEAs irradiated under identical conditions, confirming literature data that BCC structures are more resistant to hardening than FCC structures.

ACKNOWLEDGEMENTS

This work was prepared within the project № 2020.02/0327 “Fundamental aspects of the new materials creation with unique physical, mechanical and radiation properties based on the concentrated multicomponent alloys”, implemented with the financial support of the National Research Foundation of Ukraine.

REFERENCES

1. D. Stork, P. Agostini, J.L. Boutard, D. Buckthorpe, E. Diegele, S.L. Dudarev, C. English, G. Federici, M.R. Gilbert, S. Gonzalez, A. Ibarra, C. Linsmeier, A. Li Puma, G. Marbach, P.F. Morris, L.W. Packer, B. Raj, M. Rieth, M.Q. Tran, D.J. Ward, S.J. Zinkle. Developing structural, high-heat flux and plasma facing materials for a near-term DEMO fusion power plant: The EU assessment // *J. Nucl. Mater.* 2014, v. 455, p. 277-291.
2. J. Cui, Z. Cheng, D. Chen, T. Wang, L. Zhang, J. Sun. Studies on the design and properties of FeCrVTix medium-entropy alloys for potential nuclear applications // *J. Alloy. Compd.* 2022, v. 894, p. 162398.
3. D. King, A. Knowles, D. Bowden, M. Wenman, S. Capp, M. Gorley, J. Shimwell, L. Packer, M. Gilbert, A. Harte. High temperature zirconium alloys for fusion energy // *J. Nucl. Mater.* 2022, v. 559, p. 153431.

4. Y. Zhang, T.T. Zuo, Z. Tang, M.C. Gao, K.A. Dahmen, P.K. Liaw, Z.P. Lu. Microstructures and properties of high-entropy alloys // *Prog. Mater. Sci.* 2014, v. 61, p. 1-93.
5. D.B. Miracle, O.N. Senkov. A critical review of high entropy alloys and related concepts // *Acta Mater.* 2017, v. 122, p. 448-511.
6. G. Was, Z. Jiao, E. Getto, K. Sun, A. Monterrosa, S. Maloy, O. Anderoglu, B. Sencer, M. Hackett. Emulation of reactor irradiation damage using ion beams // *Scr. Mater.* 2014, v. 88, p. 33-36.
7. M.H. Tsai, J.W. Yeh. High-entropy alloys: a critical review // *Mater. Res. Lett.* 2014, v. 2, p. 107-123.
8. J.W. Yeh. Recent progress in high entropy alloys // *Ann. Chim. Sci. Mat.* 2006, v. 31, p. 633-648.
9. X.H. Yan, Y. Zhang. Functional properties and promising applications of high entropy alloys // *Scr. Mater.* 2020, v. 187, p. 188-193.
10. W.R. Zhang, P.K. Liaw, Y. Zhang. Science and technology in high-entropy alloys // *Sci. China Mater.* 2018, v. 61, p. 2-22.
11. L. Fave, M.A. Pouchon, M. Döbeli, M. Schulte-Borchers, A. Kimura. Helium ion irradiation induced swelling and hardening in commercial and experimental ODS steels // *J. Nucl. Mater.* 2014, v. 445, p. 235-240.
12. Y. Lu, H. Huang, X. Gao, C. Ren, et al. A promising new class of irradiation tolerant materials: Ti2ZrHfV0.5Mo0.2 high-entropy alloy // *Journal of Materials Science and Technology.* 2019, v. 35, p. 369-373.
13. Z. Li and D. Raabe. Strong and Ductile Non-equiatomous High-Entropy Alloys: Design, Processing, Microstructure, and Mechanical Properties // *JOM.* 2017, v. 69, N 11, p. 2099-2106.
14. O.M. Velikodnyi, R.V. Vasilenko, O.S. Kalchenko, I.V. Kolodyi, Y.O. Krainiuk, A.V. Levenets, P.I. Stoev, M.A. Tikhonovsky, G.D. Tolstolutska. Structure and mechanical properties of multicomponent Ti-Cr-Al-Nb and Ti-Cr-Al-Nb-V alloys // *PAST.* 2023, N 5(147), p. 59-67.
15. G.D. Tolstolutska, V.V. Ruzhytskiy, I.E. Kopanetz, V.N. Voyevodin, A.V. Nikitin, S.A. Karpov, A.A. Makienko, T.M. Slusarenko. Accelerating complex for study of helium and hydrogen behavior in conditions of radiation defects generation // *PAST.* 2010, N 4(65), p. 135-140.
16. <http://www.srim.org/>
17. R.E. Stoller, M.B. Toloczko, G.S. Was, A.G. Certain, S. Dwaraknath, F.A. Garner. On the use of SRIM for computing radiation damage exposure // *Nucl. Instr. Methods Phys. Res. B.* 2013, v. 310, p. 75-80.
18. G.N. Tolmachova, G.D. Tolstolutska, S.A. Karpov, B.S. Sungurov, R.L. Vasilenko. Application of nanoindentation for investigation of radiation damage in SS316 stainless steel // *PAST.* 2015, N 5(99), p. 168-173.
19. W.C. Oliver, G.M. Pharr. An improved technique for determining hardness and elastic modulus using load and displacement sensing indentation experiments // *J. Mater. Res.* 1992, v. 7 (6), p. 1564-1583.

20. W.D. Nix, H.J. Gao. Indentation size effects in crystalline materials: A law for strain gradient plasticity // *J. Mech. Phys. Solid.* 1998, v. 46, p. 411-425.
21. A. Kareer, A. Prasitthipayong, D. Krumwiede, D.M. Collins, P. Hosemann, S.G. Roberts. An analytical method to extract irradiation hardening from nanoindentation hardness-depth curves // *J. Nucl. Mater.* 2018, v. 498, p. 274-281.
22. S.A. Karpov, G.D. Tolstolutskaia, V.N. Voyevodin, G.N. Tolmachova, I.E. Kopanets. The dose dependence of inert gases irradiation hardening of 316 austenitic stainless steel after low temperature irradiation // *PAST.* 2018, N 5(117), p. 34-39.
23. R. Kasada et al. A new approach to evaluate irradiation hardening of ion-irradiated ferritic alloys by nano-indentation techniques // *Fusion Eng. Des.* 2011, v. 86, p. 2658-2661.24.
24. C.A. Schuh et al. A survey of instrumented indentation studies on metallic glasses // *J. Mater. Res.* 2004, v. 19, N 1, p. 46-57.
25. S.A. Karpov, G.D. Tolstolutskaia, B.S. Sungurov, et al. Hardening of SS316 stain-less steel caused by the irradiation with argon ions // *Mater. Sci.* 2016, v. 52, p. 377-384.
26. V.N. Voyevodin, S.A. Karpov, G.D. Tolstolutskaia, M.A. Tikhonovsky, A.N. Velikodnyi, I.E. Kopanets, G.N. Tolmachova, A.S. Kalchenko, R.L. Vasilenko, I.V. Kolodiy. Effect of irradiation on microstructure and hardening of Cr-Fe-Ni-Mn high-entropy alloy and its strengthened version // *Philos. Mag.* 2020, v. 100, p. 822-836.
27. Gary S. Was. Fundamentals of Radiation Materials Science // *Metals and Alloys.* Springer, 2016, 1002 p.
28. N.A.P.K. Kumar, C. Li, K.J. Leonard, H. Bei, S.J. Zinkle. Microstructural stability and mechanical behavior of FeNiMnCr high entropy alloy under ion irradiation // *Acta Mater.* 2016, v. 113, p. 230-244.
29. S.J. Zinkle, Y. Matsukawa. Observation and analysis of defect cluster production and interactions with dislocations // *J. Nucl. Mater. (Part A).* 2004, v. 329-333, p. 88-96.
30. E. Orowan. *Internal Stresses in Metals and Alloys.* Institute of Metals, London, 1948, p. 451.
31. A. Seeger. *Proceedings of the 2nd International Conference on Peaceful Uses of Atomic Energy.* Geneva, vol. 6, International Atomic Energy Agency, Vienna, Austria, 1958, p. 250.
32. M. Sadeghilaridjani, A. Ayyagari, S. Muskeri, V. Hasannaemi, R. Salloom, W.-Y. Chen, S. Mukherjee. Ion irradiation response and mechanical behavior of reduced activity high entropy alloy // *J. Nucl. Mater.* 2020, v. 529, p. 151955.
33. G. Velis, M.W. Ullah, H. Xue, K. Jin, M.L. Crespillo, H. Bei, W.J. Weber, Y. Zhang. Irradiation-induced damage evolution in concentrated Ni-based alloys // *Acta Mater.* 2017, v. 135, p. 54-60.
34. M.W. Ullah, D.S. Aidhy, Y. Zhang, W.J. Weber. Damage accumulation in ion-irradiated Ni-based concentrated solid-solution alloys // *Acta Mater.* 2016, v. 109, p. 17-22.
35. A.N. Velikodnyi, V.N. Voyevodin, A.S. Kalchenko, S.A. Karpov, I.V. Kolodiy, M.A. Tikhonovsky, G.D. Tolstolutskaia, F.A. Garner. Impact of nano-oxides and injected gas on swelling and hardening of 18Cr10NiTi stainless steel during ion irradiation // *J. Nucl. Mater.* 2022, v. 565, p. 153666.
36. Shi-Hao Lia, Jian Zhang, Wei-Zhong Han. Helium bubbles enhance strength and ductility in small-volume Al-4Cu alloys // *Scripta Materialia.* 2019, v. 165, p. 112-116.
37. Yongqin Chang, Jing Zhang, Xiaolin Li, Qiang Guo, Farong Wan, Yi Long. Microstructure and nanoindentation of the CLAM steel with nanocrystalline grains under Xe irradiation // *J. Nucl. Mater.* 2014, v. 455, p. 624-629.
38. C.R. Lear, J.G. Gigax, O. El Atwani, M.R. Chancey, H. Kim, N. Li, Y. Wang, S.J. Fensin. Effects of helium cavity size and morphology on the strength of pure titanium // *Scripta Materialia.* 2022, v. 212, p. 114531.
39. J. Henry, M.-H. Mathon, P. Jung. Microstructural analysis of 9%-Cr martensitic steels containing 0.5 at.% helium // *J. Nucl. Mater.* 2003, v. 318, p. 249-259.
40. Z. Cheng, J. Sun, X. Gao et al. Irradiation effects in high-entropy alloys and their applications // *J. Alloy. and Compounds.* 2023, v. 930, p. 166768.

Article received 02.09.2023

ЗМІЦНЕННЯ ЛЕГКИХ БАГАТОКОМПОНЕНТНИХ СПЛАВІВ НА ОСНОВІ ТИТАНУ ПІД ДІЄЮ ОПРОМІНЮВАННЯ ІОНАМИ Ar

Г. Толстоуцька, М. Тихоновський, О. Великодний, С. Карпов, В. Ружицький,
Г. Толмачова, Р. Василенко

Серед нових перспективних матеріалів в останні роки значну увагу привертають багатокомпонентні сплави (БКС) завдяки їхній відмінній корозійній та радіаційній стійкості, а також високим механічним властивостям у широкому діапазоні температур. Досліджено нові легкі БКС на основі титану 61Ti-10Cr-7Al-11V-11Nb (ат. %) з високою пластичністю при кімнатній та підвищених температурах. Ці однофазні об'ємноцентровані кубічні (ОЦК) сплави опромінювали іонами Ar з енергією 1,4 MeV при кімнатній температурі до доз середнього діапазону від 1 до 10 змишень на атом. Вплив опромінення вивчався шляхом дослідження зміцнення. Було проведено порівняння з індукованим опроміненням зміцненням Ti-БКС, аустенітної нержавіючої сталі 316, гранецентрованого кубічного (ГЦК) високоентропійного сплаву, опроміненних за ідентичних умов. Показано, що твердість зростає зі збільшенням дози опромінення для всіх досліджуваних матеріалів, але це зростання є меншим у багатокомпонентних сплавах як ГЦК-, так і ОЦК-структур, ніж у звичайній нержавіючій сталі.